Astron. Astrophys. 265, 32–39 (1992)

ASTRONOMY AND ASTROPHYSICS

The radial structure of the galactic disc*

Annie C. Robin[1,2], Michel Crézé[2], and Vijay Mohan[3]

[1] Observatoire de Besançon, BP1615, F-25010 Besançon Cedex, France
[2] CNRS URA1280, Observatoire de Strasbourg, 11 rue de l'Université, F-68000 Strasbourg, France
[3] U.P. State Observatory, Manora Peak, Nainital, 263129 India

Received May 20, accepted July 20, 1992

Abstract. Three colour photometry on CCD frames in the Special Area SpA23 provides a deep probe of the galactic disc in a low absorption window towards the anticenter. Magnitudes to better than 10% at V = 25 and B-V colour down to V = 23 have been obtained. These new data, used in combination with lower magnitude photographic data in a wider field, give a strong evidence that the galactic density scale length is rather short (2.5 kpc) and drops abruptly beyond 6 kpc.

Key words: galactic structure – stellar populations – galactic disc – anticenter – photometry

1. Introduction

Currently accepted ideas concerning the structure and evolution of stellar populations in our Galaxy are mainly based on detailed observations of stars in the close solar neighbourhood. The raw observational data which can be obtained for many faint stars do not allow deriving intrinsic stellar parameters such as distance, mass, age, evolutionary stage, chemical composition, interstellar extinction of individual stars. However, some information relevant to the distribution of these quantities is reflected in the n-dimensionnal distribution of observables. Magnitudes and colours are also connected to ages and star formation processes through the history of star formation and evolution. Connecting observable distributions to the main processes they come from is basically a multivariate problem for which we have developed at the Observatoire de Besançon both a synthetic approach of Galaxy modelling (hereafter referred to as the Besançon model, Robin & Crézé 1986; Bienaymé et al. 1987) and a multivariate sample survey plan including complete samples of UBV photometry and proper motions in a set of galactic fields.

Mohan et al. (1988) performed UBV star counts on Schmidt plates in the direction of the Special Selected Area (SpA23) near the galactic anticenter. The selected field was identified by Kapteyn as a low extinction window. Mohan's observations are complete in U-B and B-V down to V magnitude 16.5. This intermediate magnitude sample was shown to provide tight constraints for the disc scale length and the local extinction. Going to deeper magnitudes gives the possibility to probe the stellar populations further away from the Sun, giving access to the disc edge, and to test intrinsically fainter populations (K and M dwarfs, white dwarfs). This paper is dedicated to processing deeper probes in this direction (SpA23, $l = 179°, b = 2.5°$). CCD photometry is obtained in three photometric bands close to the Johnson UBV system down to magnitudes as faint as 25 in V.

2. CCD photometry

2.1. Photometric system

CCD observations have been obtained with the 3.6 meter Canada-France-Hawaii Telescope. We have used the RCA2 CCD along with the wide field corrector at the prime focus, giving a scale of 13.9"/mm. The dimensions of the chip are 640x1024 pixels, which correspond to about 8 square arcminutes. To improve the statistics we have observed 4 neighbouring fields giving a survey area 29 arcmin^2. The UBV filters have been selected to match as closely as possible the Johnson system, even at the expense of loss of sensitivity. The filters used were:

V : CFHT Mould V
B : CFHT B2 (BG12-2mm, BG18-2mm, GG385-2mm)
U : UG1 + CuSO4.

The B filter has been chosen so that, when multiplied by the spectral response of the CCD, it produced a passband as close as possible to the Johnson B filter. This caused a certain loss of transmittence, but resulted in a colour coefficient close to unity. The colour equations to convert the instrumental system to the Johnson one have been computed by Mohan et al. (1988). They are:

$$V = v \tag{1}$$

$$B - V = 1.06(b - v) - 0.68 \tag{2}$$

$$U - B = 1.36(u - b) - 1.92 \tag{3}$$

2.2. Data reduction

In each field a large number of short exposures have been taken alternatively with standard field exposures, allowing to obtain an absolute calibration and to measure the air mass corrections. Long exposures have been recoordinated and summed. Long exposure data are given in Table 1. We totalise about 1H40mn in V, 2h in B and 3 to 3h30 in U in each field.

Send offprint requests to: A.C. Robin
*Based on observations made at Canada-France-Hawaii Telescope reduced using the ESO-MIDAS and DAOPHOT software packages

Table 1. Field coordinates and exposure times in seconds in each field.

Field	RA (1950)	Dec (1950)	l	b	V	B	U	Dates
1	5 53 06.5	+30 39 43	179.70	2.88	7200	6300	13076	jan 1987, jan 1988
2	5 52 45.4	+30 40 52	179.64	2.83	6000	6300	10800	jan 1988
3	5 52 54.7	+30 36 13	179.73	2.82	6000	7200	10800	jan 1988
4	5 52 46.4	+30 38 24	179.68	2.81	6000	7200	10560	jan 1988

The image processing was carried out using the DAOPHOT software package (Stetson 1987) in the ESO-MIDAS environment. First, stars were detected above a given threshold and stored in a catalogue of stars with positions, estimated magnitudes, roundness and sharpness according to the mean FWHM. Then aperture photometry was performed for each detected star. A point spread function (PSF) was computed by choosing isolated stars in the field. The number of PSF stars was of the order of 10 to 12 for short exposures and 15 to 25 for long exposures. Most of the time we found enough isolated stars such that we did not need to iterate the process (by subtracting neighbouring stars using the first guessed PSF and recomputing it with new isolated stars). Finally magnitudes were computed by fitting the PSF to each star through an iterative process. The resulting magnitudes were then shifted to the aperture magnitude by a constant computed with the isolated stars.

The CCD magnitudes on short exposure frames were calibrated using the photometric sequence of the region S241 (Moffat et al. 1979) and NGC2301 (Hoag et al. 1961). The S241 sequence was observed several times during each night in alternance with fields 1 and 2 in each filter and at different airmasses. The list of standards has been given in Mohan et al. (1988), Table 9. Extinction slopes have been computed to get magnitudes outside the atmosphere. Fields 3 and 4 were calibrated using fields 1 and 2 as standards. Colour equations were then used to transform the magnitudes to the Johnson system. Finally long exposures were calibrated differentially with short exposures in each field. The photometric accuracy has been estimated by comparison of the magnitudes measured on various exposures. Table 2 gives the estimated accuracy as a function of magnitude down to the completeness limit in each band. It should be noted that the accuracy degrades at bright magnitudes because the PSF is distorted and that at faint magnitudes the degradation depends on the seeing. In the U band it seems that at faint magnitudes stars are lost before the accuracy get less than 0.1.

In this reduction process dedicated to crowded fields, the galaxies are lost, while some are visible in two of our fields.

Table 2. Estimated photometric accuracy as a function of magnitude in each band

Magnitude	V	B	U
18-19	0.02	0.02	0.02
19-20	0.01	0.02	0.02
20-21	0.02	0.01	0.01
21-22	0.02	0.01	0.01
22-23	0.04	0.03	0.01
23-24	0.05	0.04	0.04
24-25	0.08	0.09	

2.3. Detection limit and completeness limit

Stars are detected to very faint magnitudes (28 in V) but they are measured with a very poor accuracy. They are not useful since their brightness is measured with an accuracy of the order of one magnitude or more. For our purpose we need a catalogue with a very well defined completeness limit. Stars are lost far before the detection limit because the signal to noise ratio degrades rapidly. The completeness failure currently appears in the magnitude histogram of any passband 2 or 3 magnitudes below the detection limit. The accuracy is better than 0.1 magnitude at 25 in V. To remain with a catalogue with a good accuracy we choose the limiting magnitude at the maximum of the histogram corresponding to an estimated error of about 0.1 magnitude. The completeness limits in each field are given in Table 3.

Table 3. Field characteristics in each photometric band : area in square arcminutes, completeness limit and estimated seeing in arcseconds

Field	Area	V		B		U	
		lim.	"	lim.	"	lim	"
1	6.7	25	1.9	22.5	1.7	22	1.7
2	6.5	25	1.8	24	1.0	22	1.3
3	7.7	25	1.3	24	1.4	21	1.3
4	6.6	25	1.6	23	1.6	23	1.5

The catalogues of position, magnitude and colours in the Johnson system of the stellar objects brighter than 25 in V are available at the Centre de Donnees astronomiques de Strasbourg (CDS) or on request.

3. Model fitting

While a global analysis of all program fields is necessary to tune our model to reality, a field by field analysis should be performed first to evaluate primary values of important parameters. Also, eye comparisons help in estimating the quality of model predictions. In the following we first determine the interstellar extinction in this field from the U-B,B-V distribution, then we deduce the density law characteristics of the stellar populations towards the anticenter.

3.1. (U-B, B-V) diagrams

The number of stars in each field with a measured U-B colour index (about 40 to 50) allows to estimate the mean reddening for stars with V less than about 21 using colour- colour diagrams. Since the main sequence is nearly parallel to the reddening line in the U-B/B-V diagram, the measure of the reddening by fitting a shifted main sequence is rather inaccurate. We prefer to properly

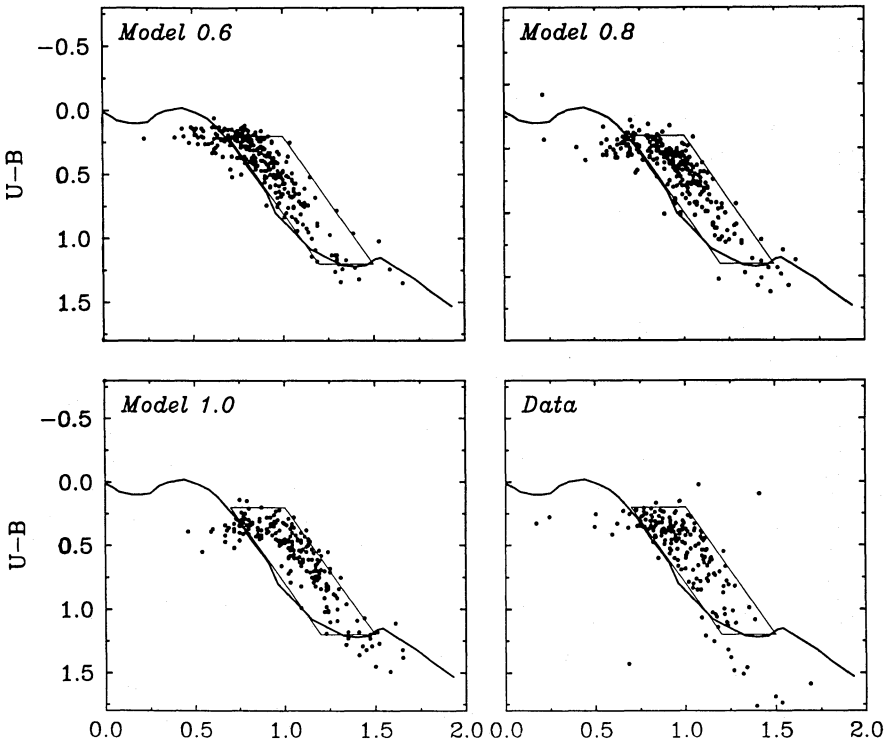

Fig. 1. Model simulated U-B vs B-V diagram reddened by different values of local differential absorption. a) 0.6 magnitude per kiloparsec. b) 0.8. c) 1.0. The reference sequence (solid line) is the unreddened main sequence. d) Observed diagram plotted over the unreddened main sequence (solid line). A visual guide has been printed as a parallelogram where most of the stars are.

model the extinction using our model of population synthesis which will be used to interpret the stellar statistics. The model has been extensively described in Robin, Crézé (1986) and in Bienaymé et al. (1987).

In the model simulated star counts, we try various density distributions of the absorbing material. An Einasto law (Einasto 1977; see also Sect. 3.2 below) has been used to model the absorbing layer as a disc quite similar to the youngest stars'. In addition to this smooth distribution absorbing clouds can be introduced as well along the line of sight. The amount of local differential absorption may be either tuned to the data or estimated using maps of interstellar matter. A value of 0.7 magnitude per kiloparsec is suitable for fields at intermediate and high galactic latitude.

Mohan et al. (1988) determined the absorption law in SpA23 field from their Schmidt data. They found a value of 0.7 magnitude per kiloparsec from stars of magnitude 12 to 16. Since the bulk of CCD stars, ranging between 17 and 25 are on the average more distant, the absorption law should be reinvestigated.

Using the same method we estimate the mean interstellar extinction in the four fields simultaneously. To reduce the number of parameters, the extinction law is assumed not to vary within the 5' by 5' joint fields. Figure 1 shows a set of model predicted diagrams based on three values of diffuse absorption from 0.6 to 0.9 magnitude per kpc together with the unreddened main sequence. Matching simulated diagrams to observed ones in different V magnitude intervals (visually and by computing a rms estimation of the agreement) gives a best fit value of 0.8 ± 0.1 magnitude per kiloparsec for the local differential visual extinction and $A_V = 1.2 \pm 0.15$ at 4 kpc. Figure 1d shows the observed two-colour diagram of stars in the 4 CCD fields alongwith the unreddened main sequence. Finally we give in Table 4 the mean distance and colour excess of model stars in each magnitude bin, assuming that the ratio between the visual absorption and the reddening is 3.0 as suitable for dwarfs stars. These average points are plotted in Fig. 2 over a set of model absorption curves.

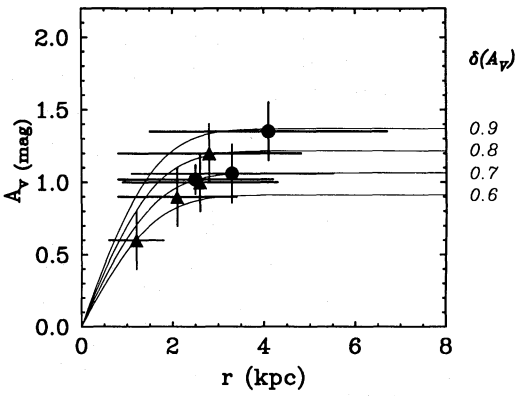

Fig. 2. Distribution of interstellar extinction along the line of sight. Estimated values from (U-B, B-V) diagrams from CCD (full circles), from Schmidt plates (triangles), and model with differential local absorption between 0.6 and 0.9 mag. kpc^{-1} (thin lines).

3.2. Global extinction in the field

In the 4 CCD frames a number of galaxies are easily distinguishable. Among the brightest we identify 4 ellipticals which can help to determine the overall extinction in the Galaxy since they have

Table 4. Estimation of the interstellar reddening in each magnitude bin from the U-B/B-V diagrams to V=21. Mean distance and dispersion of subsample stars are given in columns 5 and 6. Column 7 is the model predicted A_V (best fit) at the mean distance.

Data	Magnitude Intervalle	E(B-V)	A_V	Mean d (kpc)	σ(d)	$A_{V,model}$
Schmidt	12-13	0.2	0.6	1.2	0.6	0.8
	14-15	0.3	0.9	2.1	1.3	1.1
	15-16	0.33	1.0	2.6	1.7	1.2
	16-16.5	0.40	1.2	2.8	2.0	1.2
CCD	15-17	0.34	1.02	2.5	1.7	1.2
	17-19	0.35	1.06	3.3	2.2	1.2
	19-21	0.45	1.35	4.1	2.6	1.2

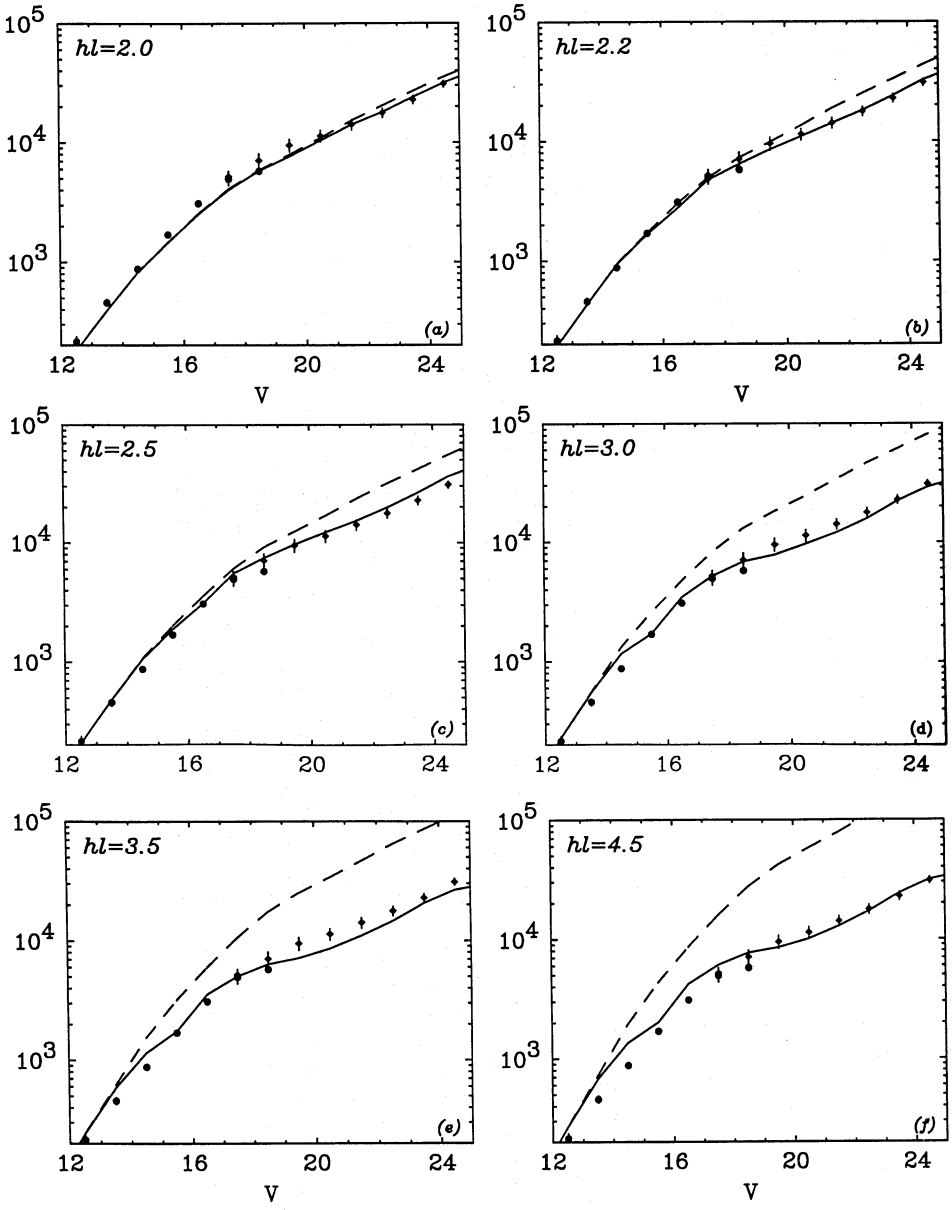

Fig. 3. Distribution in V. Schmidt data (circles), CCD data (diamonds), models with various scale lengths : hl=2.0 (a), 2.2 (b), 2.5 (c), 3.0 (d), 3.5 (e), 4.5 (f). Solid line: model density laws with best fit cutoff (9.5, 6.5, 4.5, 4.0, 3.5, 3.0 kpc resp.); dashed line: model density laws assuming no cutoff.

quite well defined intrinsic colors (de Vaucouleurs 1976) B-V = 0.9 ± 0.1 and U-B = 0.45 ± 0.15.

The V magnitude and B-V colour have been measured for the 4 ellipticals as well as U-B for the brightest. We deduce the B-V excess according to supposed intrinsic colours (Table 5). The values are slightly higher than the reddening determined from the UBV diagram but are within the measuring errors. Only one galaxy shows a significantly higher extinction.

Table 5. Colours of ellipticals measured in the CCD fields. E(B-V) is the reddening in front of the galaxies assuming intrinsic B-V of 0.9 .

field	Id	V	B-V	U-B	E(B-V)	σ	A_V
2	1	18.40	1.42	0.66	0.52	0.10	1.56
2	2	21.46	1.46	-	0.56	0.15	1.68
4	3	21.78	1.62	-	0.72	0.15	2.16
4	4	22.12	1.49	-	0.59	0.15	1.77

Previous estimations of the amount of absorption in anticenter fields close to ours led to similar results. SpA23 is at the limit between two zones investigated by Neckel & Klare (1980). They estimate the total visual extinction between 0.5 and 1.2 in the first zone, and between 1.2 and 1.9 in the second one. It is well in agreement with the presently determined value of 1.2 ± 0.15.

McCuskey (1967) gives A_V = 1.8 mag. at 2 kpc and 2.3 at 4 kpc in a field at $l = 186°, b = +1°$, significantly above our determination. However the McCuskey's field is situated at 7 degrees in longitude from SpA23 and is closer to the galactic plane. Deutschman et al. (1976) from the Celescope catalogue for quite a large region in Auriga-Gemini found values between 1.2 and 1.8 mag. of visual extinction at 3 kpc. Moreover West (1967) when studying the galactic cluster M37, located at $l = 178°$ and $b = 3°$, found an extinction of 0.8 mag. at 1450 pc. The present value of extinction at 4 kpc of 1.2 ± 0.15 and differential absorption of 0.8 ± 0.1 magnitude per kiloparsec determined independently by UBV photographic photometry on Schmidt plates and by UBV CCD photometry is thus fully compatible with the extinction measured in neighbouring fields. This is in accordance with the fact that this Kapteyn's Special Area was chosen as a zone of low extinction.

This value is also compatible with HI data in this direction which give a value of E(B-V) = 0.4.

3.3. *V, B-V data and deep V counts*

We now try to constrain the galactic structure parameters which are likely to produce a significant signature in these star counts. Apart from the extinction which has been studied above, the density law of the stellar disc must be derived mainly from counts in V and B-V, because too few stars have a measured U-B index (not fainter than 21 in V). We describe the density law towards the anticenter by two parameters, the disc scale length, hl, and the maximum distance at which we see the stars, r_{max} :

$$\rho(r) = \begin{cases} Kexp(0.5 - \sqrt{0.5^2 + (a/hl)^2}) & \text{if } r < r_{max} \\ 0. & \text{otherwise} \end{cases}$$

where $a = \sqrt{R^2 + (z/c)^2}$, R and z are the galactic coordinates and c is the axis ratio function of the age of the population, ranging from 0.02 to 0.073 in the disc. This formula gives a density equivalent to an exponential radially, while vertically it is close to a sech^2 (see Bienaymé et al. 1987, for details).

In a previous study Mohan et al. (1988) determined the disc scale length from Schmidt plate photometry completed by a preliminary reduction of CCD data of our field I to magnitude 21. The Mohan data were shown compatible only with a scale length of the order of 2.2 ± 0.3 kpc which is the value used in our standard model. The deepest and more extensive CCD samples show a change of slope which could not be detected at magnitudes brighter than 21. No satisfactory fit can now be obtained by simply fitting the disc scale length and the extinction law. A cutoff of the disc has to be introduced.

In Fig. 3 (a to f) the observed apparent magnitude distribution is compared with a series of model predictions with scale lengths ranging from 2.2 to 4.5 kpc. In each figure the model is plotted without cutoff (dashed line) and with the cutoff value resulting from the maximum likelihood estimation (solid line).

A grid of models with various scale lengths has been studied. For each of these models we determine the best value of the cutoff using a maximum likelihood technique. Since the magnitude range 12 to 16 is only slightly sensitive to the disc cutoff (as we see on Fig. 3) we use only the CCD data ranging between 16 to 25 in a first step to determine the cutoff. The likelihood for each model is computed as described in Bienaymé et al. (1987, appendix C) :

Let q_i be the number of stars predicted by the model in bin i and f_i be the observed number. In case the deviations of f_i's with respect to q_i just reflect random fluctuations in counts, each f_i would be a Poisson variate with mean q_i. Then the probability that f_i be observed is :

$$dP_i = \frac{q_i^{f_i}}{f_i!} exp(-q_i) \tag{4}$$

Then the likelihood of a set of q_i's given the relevant f_i is :

$$L = ln \sum dP_i = \sum_i (-q_i + f_i \ln q_i - \ln f_i!) \tag{5}$$

In search of the models that maximise L it is convenient to use the reduced form :

$$L - L_0 = \sum_i f_i (1 - \frac{q_i}{f_i} + ln \frac{q_i}{f_i}) \tag{6}$$

where L_0 is constant and $L - L_0 = 0$ for a model which would exactly predict all f_i's.

The likelihood computation is made in bins of V and B-V for stars having a B-V measure, that is for B less than 22.5 in all CCD fields. These data are binned with a step of 2 in V and 0.3 in B-V. Below V=20 B-V data fail to be complete in the red wing (B is complete to 22.5). Thus for some stars only V is available. To constrain the model to V=25 we add in the likelihood computation five bins of V magnitudes between 20 and 25 with a step of 1. We end up with a set of 23 bins in which the likelihood is computed. Table 6 gives the likelihood of the CCD data considering a grid of models with different scale lengths and disc cutoffs. The disc cutoff is very well determined for long scale lengths although in the case of short scale the maximum of the likelihood is wider (of course at very short scale lengths the model predictions are cutoff insensitive). However the disc scale length is not well constrained by the CCD data alone.

The bulk of stars in Schmidt data lies at relatively short distances providing a good basis to constrain the scale length

Table 6. Likelihood of CCD data under various assumed model disc scale length hl and cutoffs r_{max}.

r_{max}/hl	1.5	1.8	2.0	2.2	2.5	3.0	3.5
1.00	-1474.	-1187.	-1324.	-1316.	-1171.	- 912.	-981.
1.50	-1046.	-747.	-746.	-895.	-635.	-509.	-488.
2.00	-811.	-602.	-549.	-533.	-622.	-469.	-363.
2.50	-588.	-407.	-335.	-278.	-289.	-191.	-161.
3.00	-450.	-271.	-203.	-156.	-119.	-83.	-56.
3.50	-359.	-186.	-142.	-82.	-48.	-54.	-21.
4.00	-284.	-141.	-104.	-56.	-21.	-44.	-52.
4.50	-244.	-106.	-74.	-37.	-8.	-49.	-62.
5.00	-213.	-80.	-51.	-42.	-33.	-80.	-152.
5.50	-207.	-73.	-45.	-34.	-33.	-100.	-191.
6.00	-190.	-67.	-34.	-31.	-26.	-133.	-275.
6.50	-205.	-59.	-29.	-27.	-34.	-183.	-368.
7.00	-200.	-56.	-25.	-28.	-43.	-208.	-425.
7.50	-183.	-48.	-19.	-34.	-57.	-264.	-527.
8.00	-180.	-46.	-19.	-38.	-66.	-295.	-580.
8.50	-164.	-44.	-17.	-40.	-73.	-323.	-635.
9.00	-161.	-43.	-17.	-44.	-81.	-346.	-678.
9.50	-157.	-40.	-16.	-48.	-88.	-374.	-731.
10.00	-153.	-39.	-16.	-53.	-108.	-412.	-822.
10.50	-150.	-39.	-16.	-55.	-114.	-433.	-868.

within the first 3 kpc. Binning the Schmidt data by step of 1 magnitude in V and by 0.3 in B-V, we apply the same likelihood technique to the whole set of data (Schmidt + CCD), giving a total of 58 bins. Table 7 gives the resulting likelihoods.

The maximum likelihood is obtained with a scale length of 2.5 kpc, and a cutoff at 5.5 to 6 kpc from us. There however remains a discrepancy with the data in 8 bins in the best model. These discordant bins indicate that there may be some discrepancy in the population distribution in the HR diagram used in the present model. Since the agreement is obtained in the large majority of the bins we expect that these spurious bins would not change the conclusion about the space density of stars obtained in the overall analysis.

4. Discussion

4.1. Validity of the fitting method

The maximum likelihood is strictly valid only in so far as the space of possible models is sufficiently explored - which may not be the case if even a single important parameter has been overlooked. In our modelling the basic ingredients relevant to the interpretation of a galactic anticenter field are (i) the distribution of stars in the HR diagram (here mainly disc main sequence and few disc giants at $V < 14$) - including their age distribution, (ii) the global shape of the galactic disc (i.e. mainly the disc scale length and cutoff), (iii) the distribution of the absorbing layer.

The age distribution does not play an important role in the galactic plane since scale heights do not matter much in this low latitude field. We assumed the distribution of stars in the HR diagram to be roughly known from solar vicinity data, at least enough to be used as a standard candle to probe the external part of the galactic disc. We do not see in the data any feature that might suggest a significant effect related to spiral arms.

Under these assumptions the CCD data do provide a clear answer to the question of the disc shape : a satisfactory agreement cannot be obtained unless we impose a disc cutoff at something like 6 to 8 kpc away from the solar neighbourhood. It is remarkable that the fit to the CCD data is correct over the whole magnitude and colour range.

Once this best cutoff has been obtained for each model for the CCD data, the analysis is redone on the whole data set (CCD + Schmidt data). The best model is still the same but the likelihood degrades dramatically in some bins (which would be equivalent to a high level of rejection in a chi-square test). However the degradation is only due to a few bins - namely 8 bins out of 58, all in the Schmidt plate data. But there is no way to change the shape of the Galaxy model so as to get a better fit consistently in all bins. The same solution based only on three free parameters (scale length, single cutoff and extinction) does fit all the CCD bins, which correspond to the better known part of the main sequence (F to K dwarfs), and also the large majority of the Schmidt plate photometry.

4.2. Disc scale length

The resulting scale length of 2.5 kpc determined by our data is smaller than what is currently accepted for the galactic disc. Values obtained in the visible are of the order of 3.5 to 4.5 kpc but there are estimations ranging between 1.8 to 6 kpc. Kent et al. (1991) give a review of recent determinations. 2.2 micron determinations give quite short scale lengths (Maihara et al. (1978): 1.8 kpc; Jones et al. (1981): 2.0 kpc; Eaton et al. (1984): 3.0 kpc; Kent et al. (1991): 3.0 kpc). IRAS OH/IR star data give larger values: Habing (1988): 4.2 kpc, Rowan- Robinson & Chester(1987): 6.0 kpc. Visible data show a large spread as well: De Vaucouleurs & Pence (1978): 3.5 kpc, Lewis & Freeman (1989): 4.4 kpc, van der Kruit (1986): 5.5 kpc, Oblak & Mayor (1987): 2.5 kpc. Most such measurements are model dependent and require assumptions.

The Pioneer 10 mission has been used to map the background starlight of the Galaxy in two wavelength bands: "blue" at 395-

Table 7. Likelihood of Schmidt + CCD data under various assumed model disc scale lengths hl and cutoffs r_{max}.

r_{max} / hl	1.5	1.8	2.0	2.2	2.5	3.0	3.5
1.00	-8678.	-8168.	-7237.	-7493.	-6958.	- 5848.	-5931.
1.50	-6844.	-5577.	-4992.	-5220.	-4446.	- 3672.	-3616.
2.00	-4968.	-3808.	-3679.	-3412.	-3022.	- 2387.	-2162.
2.50	-3907.	-3015.	-2541.	-2322.	-2004.	- 1516.	-1598.
3.00	-3387.	-2368.	-1941.	-1730.	-1231.	- 987.	-1127.
3.50	-2847.	-1870.	-1427.	-1110.	-790.	- 690.	-840.
4.00	-2605.	-1624.	-1182.	-910.	-607.	- 611.	-851.
4.50	-2444.	-1453.	-1018.	-748.	-515.	- 656.	-975.
5.00	-2264.	-1264.	-831.	-636.	-461.	- 764.	-1324.
5.50	-2235.	-1212.	-786.	-592.	-444.	- 816.	-1459.
6.00	-2210.	-1139.	-705.	-529.	-438.	- 952.	-1797.
6.50	-2192.	-1086.	-683.	-513.	-492.	- 1131.	-2156.
7.00	-2164.	-1076.	-671.	-514.	-521.	- 1208.	-2321.
7.50	-2138.	-1061.	-663.	-524.	-557.	- 1328.	-2567.
8.00	-2129.	-1056.	-660.	-531.	-571.	- 1384.	-2658.
8.50	-2111.	-1052.	-658.	-536.	-583.	- 1435.	-2753.
9.00	-2107.	-1051.	-659.	-540.	-596.	- 1476.	-2828.
9.50	-2101.	-1047.	-657.	-547.	-608.	- 1514.	-2907.
10.00	-2096.	-1044.	-657.	-555.	-633.	- 1562.	-3033.
10.50	-2093.	-1040.	-658.	-556.	-640.	- 1589.	-3095.

485 nm and "red" at 590-690 nm. A scale length of 5.5 kpc has been deduced from the Pioneer data by van der Kruit (1986) through a number of assumptions. The Bahcall & Soneira model (1984) was used to deconvolve data since only integrated surface brightness over the line of sight was available. The comparison between model and data led to major problems (model too bright at high latitudes, too big slope in the profile and too faint at intermediate latitudes) and a rescaling of the local luminosity density of the model was necessary to fit the data. It is difficult to estimate the effect of such a rescaling on the resulting scale length. Moreover, Pioneer data do not constrain directly the scale length but the ratio $\frac{hl}{hz}$ such that the results depend on the assumed scale height. They emphasized a value of 325 pc (that is the value of old disk dwarfs) while one expects that old disk giants would dominate the light in Pioneer data (Lewis & Freeman 1989). Lewis & Freeman (1989) determined the radial scale length from the kinematics of disk K giants. They found a different scale for σ_R and for σ_ϕ (4.4 and 3.4 kpc respectively). These values should depend on assumptions on the axisymmetry of the Galaxy.

The measurement of the asymmetric drift gives an alternative to determine the radial scale length. It depends on the sum of the radial density gradient and the velocity dispersion gradient $\frac{\partial ln\rho}{\partial R} + \frac{\partial ln\sigma_U^2}{\partial R}$.

Mayor (1974) found -0.65 kpc^{-1} for the total value using a sample of 1010 A and F stars with uvby photometry. The value of the velocity dispersion gradient may be determined using the stability criterion of the galactic disc introduced by Toomre (1964). In a Schmidt model (1965) Mayor deduced a value of -0.2 for $\frac{\partial ln\sigma_U^2}{\partial R}$ in contrast to the value of 0 that one would have in the ellipsoidal hypothesis. This result has been confirmed by Oblak & Mayor (1987) from F, G and K type stars in the Gliese catalogue who found values between -0.14 and -0.24. It is also in good agreement with the estimation of Vandervoort (1975) and Erickson (1975) based on the 3rd and 4th order moments of the local stellar velocity distribution (between −0.19 and −0.23 kpc $^{-1}$).

The radial density gradient $\frac{\partial ln\rho}{\partial R}$ implied by these values is −0.45 kpc $^{-1}$ corresponding to a scale length of 2.2 kpc, in perfect agreement with our measurement.

4.3. The edge of the galactic disc

The disc cutoff has been found at a quite short distance (6 kpc), giving a galactic radius of 14 to 15 kpc. Habing (1988) found a cutoff at even shorter distances (between 1 and 2.5 kpc) from the study of OH/IR stars from the analysis of the IRAS Point Source Catalogue. However the model he used was based on a disc scale length of 4.5 kpc, quite larger than ours. Moreover Habing mentionned that these parameters were not strongly constrained by his data and that a number of slightly different models would also be compatible with these IRAS data. It would be interesting to verify that our present measures of the disc scale length and cutoff are compatible with Habing's analysis.

While our measurement is compatible with a rather sharp cutoff at the edge of the disc it might be slightly smoother according to the population studied. Remote open clusters have been found at quite large distances in the anticenter (Be 21 at 14.5 kpc from the center and To 2 at 16 kpc, Janes 1991) which is not incompatible with our result.

4.4. Star distribution in the HR diagram

Among the 58 bins where there are stars in the (V,B-V) grid, 8 bins show a significant difference between the number of stars predicted and the observed one. The interpretation that comes out is that the frequency of stars in the parts of the HR diagram which correspond to these bins is not realistic. They correspond to 4 zones:

(i) $12 < V < 14$ and $B - V < 0.3$: These stars are A and F stars of absolute magnitude 0. to 1., and too many are produced by the model. This may call into question the adopted dwarf to

giant ratio in this part of the HR diagram computed from the Michigan catalogue.

(ii) $12 < V < 13$ and $0.6 < B-V < 0.9$: They are G subgiants lacking in the model by a factor of 2. Their absolute magnitude has been adopted to be 3. There are some suggestions that this magnitude could be slightly too bright (Grenon, private communication). Since they have been computed from local counts the inferred local density depends strongly on the assumed absolute magnitude (see below). A further study of the subgiant absolute magnitude and local density would clarify this point.

(iii) $15 < V < 16.5$ and $0.3 < B-V < 0.6$: These stars are F stars of absolute magnitude 1 to 3.5 which are lacking in the model. This point may be related to the dwarf to subgiant ratio (see above).

(iv) $14 < V < 16.5$ and $1.2 < B-V < 1.5$: Too many K giants are produced by the model in these bins. This problem has already been addressed (Robin 1989). We showed that the absolute magnitudes of K giants are very uncertain because for a given spectral type a large dispersion in absolute magnitude is in fact observed (the so called 'funnel effect'). The mean magnitude obtained is very much dependent on the selected sample.

In our approach the number of giants (and subgiants) predicted is very sensitive to the assumed absolute magnitude since we recompute their local density from the distribution of these stars in the solar neighbourood. An error of 0.5 magnitude on M_V implies an error of a factor 2 on the sampling volume, hence on the computed local density. Our present estimate of absolute magnitude is good to about 0.5 magnitude only. We need to model in more detail this part of the HR diagram (accounting in detail for the mixing of stars of various ages and masses) to be able to fit perfectly those star counts. The Hipparcos mission would be able to partly solve this problem - at least for the estimation of the absolute magnitudes. However, the problem of mixing stars of different types in the same part of the HR diagram will remain, until we have better stellar evolution models.

However, we hope that while studying in detail the (V,B-V) distribution of the stars, we will be able to constrain the stellar distribution in the HR diagram with a better accuracy than is presently achievable.

5. Conclusion

We have combined star count data towards the anticenter using Schmidt Plates and CCD frames to constrain a model of galatic structure. Thus we probe a magnitude range from 10 to 25 in V, with two colour indices for stars with $V \leq 21$ and one colour index to magnitude 23. We are able to determine the extinction law from the (V,U-B,B-V) data cube and to deduce the disc scale length and cutoff. In the anticenter direction the disc shows quite a short scale length of 2.5 kpc and the stellar density drops abruptly beyond 6 kpc.

This drop cannot be explained by the existence of a dense cloud causing interstellar extinction because the U-B,B-V stellar data, as well as the colours of 4 elliptical galaxies in the field, exclude a large amount of extinction.

Stars counted on CCD frames should have absolute luminosities between 4 and 13 (M_V) while those dominating Schmidt plate counts range between 0 and 5. A complete ad hoc revision of the luminosity function from 0 to 13 would be necessary in order to get a reasonable fit over the whole V distribution. So there is no realistic change of the luminosity function that might produce a fit over the whole magnitude range.

Acknowledgements. This research was partially supported by the Indo-French Centre for the Promotion of Advanced Research / Centre Franco- Indien Pour la Promotion de la Recherche Avancée.

References

Bahcall, J.N., Soneira, R.M. 1984, ApJS, 55, 67
Bienaymé, O. Robin, A.C., Crézé, M. 1987, A&A, 180, 94
Deutschman, W.A., Davis, R.J., Schild, R.E. 1976, ApJS, 30, 97
de Vaucouleurs, G. 1976, Le Monde des Galaxies, A. Hayli (ed), Observatoire de Besançon
de Vaucouleurs G., Pence, W.D. 1978 , AJ, 83, 1163
Eaton, N, Adams, D.J., Giles, A.B. 1984, MNRAS, 208, 241
Einasto, J. 1977, IAU Symp. 84, The large Scale Characteristics of the Galaxy, ed. W.B. Burton, p. 451
Erickson, R.R. 1975, ApJ, 195, 343
Habing, H.J. 1988, A&A, 200, 40
Hoag, A.A., Johnson, H.L., Iriarte, B., Mitchell, R.I., Hallman, K.L., Sharpless, S. 1961, Publ. U.S. Nav. Obs., 17, part 7
Janes, K.A. 1991, Precision Photometry, A.G.D. Philip, A.R. Upgren and K.A. Janes (eds), L. Davis Press, p. 233
Jones, T.J., Ashley, M., Hyland, A.R., Ruelas-Mayorga, A. 1981, MNRAS, 97, 413
Kent, S.M., Dame, T.M., Fazio, G. 1991, ApJ, 378, 131
Lewis J.R., Freeman, K.C. 1989, AJ, 97, 139
Maihara, T., Oda, N., Sugiyama, T., Okuda, H. 1978, PASJ, 30, 1
Mayor, M. 1974, A&A, 32, 321
McCuskey, S.W. 1967, AJ, 72, 1199
Moffat, A.F.J., Fitzgerald, M.P., Jackson, P.D. 1979, A&AS, 38, 197
Mohan, V., Bijaoui, A., Crézé, M., Robin, A.C. 1988, A&AS, 73, 85
Neckel, Th., Klare, G. 1980, A&AS, 42, 251
Oblak, E., Mayor, M. 1987, Evolution of Galaxies, X IAU European Meeting, J. Palous (ed), Publ. Astron. Inst. Czech. Acad. Sci. 69, 263
Robin, A.C., Crézé, M. 1986, A&A, 157, 71
Robin, A.C., 1989 A&A, 225, 69
Rowan-Robinson, M. Chester, T. 1987, ApJ, 313, 413
Schmidt, M.: 1965, Stars and Stellar Systems, Vol. V, Ed. A. Blaauw and M. Schmidt, Univ. of Chicago Press, p. 513
Stetson, P.B. 1987, PASP, 99, 191
Toomre, A. 1964, ApJ, 139, 1217
Vandervoort, P.O. 1975, ApJ, 195, 333
van der Kruit, P.C. 1986, A&A, 157, 230
West, F.R. 1967, ApJS, 14, 359

This article was processed by the author using Springer-Verlag LaTeX A&A style file 1990.